Appl Microbiol Biotechnol (2016) 100:6725–6737
DOI 10.1007/s00253-016-7565-x

Improvement of DNA minicircle production by optimization of the secondary structure of the 5′-UTR of ParA resolvase

Michaela Šimčíková[1,2,3] · Cláudia P. A. Alves[1] · Liliana Brito[1] · Kristala L. J. Prather[2,3,4] · Duarte M. F. Prazeres[1,2,3] · Gabriel A. Monteiro[1,2,3]

Received: 21 March 2016 / Revised: 8 April 2016 / Accepted: 16 April 2016 / Published online: 5 May 2016

Abstract The use of minicircles in gene therapy applications is dependent on the availability of high-producer cell systems. In order to improve the performance of minicircle production in *Escherichia coli* by ParA resolvase-mediated in vivo recombination, we focus on the 5′ untranslated region (5′-UTR) of *parA* messenger RNA (mRNA). The arabinose-inducible P_{BAD}/araC promoter controls ParA expression and strains with improved arabinose uptake are used. The 27-nucleotide-long 5′-UTR of *parA* mRNA was optimized using a predictive thermodynamic model. An analysis of original and optimized mRNA subsequences predicted a decrease of 8.6–14.9 kcal/mol in the change in Gibbs free energy upon assembly of the 30S ribosome complex with the mRNA subsequences, indicating a more stable mRNA-rRNA complex and enabling a higher (48–817-fold) translation initiation rate. No effect of the 5′-UTR was detected when ParA was expressed from a low-copy number plasmid (~14 copies/cell), with full recombination obtained within 2 h. However, when the *parA* gene was inserted in the bacterial chromosome, a faster and more effective recombination was obtained with the optimized 5′-UTR. Interestingly, the amount of this transcript was 2.6–3-fold higher when compared with the transcript generated from the original sequence, highlighting that 5′-UTR affects the level of the transcript. A Western blot analysis confirmed that *E. coli* synthesized higher amounts of ParA with the new 5′-UTR (~1.8 ± 0.7-fold). Overall, these results show that the improvements made in the 5′-UTR can lead to a more efficient translation and hence to faster and more efficient minicircle generation.

Keywords Minicircle · *parA* resolvase · 5′-UTR · Ribosome binding site · mRNA secondary structure · Translational initiation rate

Introduction

The low efficacy of plasmids as gene transfer vectors in gene therapy and DNA vaccination applications has been attributed to several reasons, including (i) low cell and nucleus uptake (Kreiss et al. 1999; Dean et al. 2005), (ii) degradation by endogenous nucleases during cytoplasm trafficking (Lechardeur et al. 1999; Azzoni et al. 2007), and (iii) silencing of transgene expression (Faurez et al. 2010; Lu et al. 2012). As a result, plasmid-mediated transgene expression is usually short-lived and gene delivery falls short of its goal. Furthermore, and although plasmids have a very good safety record in the clinic, concerns regarding the induction of unwanted immunogenic reactions (Zhao et al. 2004) and integration into the host genomic DNA (Wang et al. 2004) are recurrent. These events have been linked in part to the presence in the plasmid vector backbone of DNA sequences such as promoters, un-methylated cytosine-phosphate-guanine (CpG) motifs, or selection markers, which are mostly of bacterial origin. For example, bacterial DNA sequences have

Electronic supplementary material The online version of this article (doi:10.1007/s00253-016-7565-x) contains supplementary material, which is available to authorized users.

✉ Gabriel A. Monteiro
gabmonteiro@tecnico.ulisboa.pt

[1] iBB—Institute for Bioengineering and Biosciences, Department of Bioengineering, Instituto Superior Técnico, Universidade de Lisboa, Av. Rovisco Pais, 1049-001 Lisbon, Portugal

[2] MIT-Portugal Program, Cambridge, MA, USA

[3] MIT-Portugal Program, Lisbon, Portugal

[4] Department of Chemical Engineering, Massachusetts Institute of Technology, Cambridge, MA, USA

been shown to play a role in the silencing of plasmid-mediated transgene expression (Chen et al. 2004; Chen et al. 2008). Additionally, CpG motifs of bacterial origin found in most plasmid vectors are known to drive inflammatory responses. While this property can be advantageously explored when the generation of an adaptive response to a given antigen is being sought (e.g., in the case of DNA vaccines, Chen et al. 2011), such inflammatory responses may be strong enough to cause severe adverse effects (Zhao et al. 2004). Thus, the removal of CpG motifs from a plasmid vector can substantially improve both safety and the duration of the expression of the encoded therapeutic function (Yew et al. 2002). Additionally, the antibiotic selection marker used to select plasmids during production may in some cases increase the risk of spread of antibiotic resistance traits to environmental microbes (EMA 2001; USFDA 2007; Salyers et al. 2004). Finally, cryptic eukaryotic transcription signals naturally occurring in plasmid backbones may give rise to deviant transcripts and unanticipated RNA processing that alter gene activity (Bert et al. 2000; Lemp et al. 2012). Although essential for selection and replication in microbial host cells (e.g., *Escherichia coli*) during manufacturing, most of the sequences described above are superfluous in terms of the eukaryotic gene expression that is at the heart of gene therapy and DNA vaccination applications.

Minicircles are plasmid-derived, covalently closed double-stranded DNA molecules that do not contain the bacterial elements required for selection and amplification. Since they comprise exclusively the eukaryotic expression cassette, minicircles exhibit increased transfection efficiency and transgene expression when compared to their parental plasmids on an equimolar basis (Darquet et al. 1997; Darquet et al. 1999; Kreiss et al. 1998; Mayrhofer et al. 2008; Mayrhofer et al. 2009). The typical minicircle production scheme encompasses an in vivo induced recombination event between two direct repeats within a parental plasmid. This event originates two supercoiled plasmid DNA molecules: (i) a minicircle that carries the eukaryotic expression cassette and (ii) a replicative miniplasmid that contains the bacterial elements required for amplification. Various recombinases acting under the regulation of inducible promoters have been used to catalyze the excision and ligation of the minicircle sequences from parental plasmids. For example, the phage λ integrase (Darquet et al. 1997; Darquet et al. 1999; Kreiss et al. 1998) is induced by a thermal shift to 42 °C from the cI857 promoter, whereas Cre recombinase (Bigger et al. 2001), ϕC31 integrase (Chen et al. 2003; Chen et al. 2005; Kay et al. 2010), and ParA resolvase (Jechlinger et al. 2004; Mayrhofer et al. 2005; Kobelt et al. 2013) are all regulated from a P_{BAD}/araC expression system. The first attempts to produce minicircles relied on a single copy of a recombinase gene placed on the chromosome of the host and yielded relatively low recombination efficiencies (<60 %) (Darquet et al. 1997; Darquet et al. 1999; Kreiss et al. 1998; Bigger et al. 2001). Later, a number of researchers showed that complete recombination could be achieved if each parental plasmid encoded its own recombinase (Chen et al. 2003; Jechlinger et al. 2004; Chen et al. 2005; Mayrhofer et al. 2005). Complete recombination of parental plasmid from the chromosome is also feasible if expression is driven by more than one gene copy, as demonstrated by the use of ten copies of the ϕC31 integrase in the *E. coli* strain ZYCY10P3S2T (Kay et al. 2010).

The application of minicircles in the fields of DNA vaccination and gene therapy is currently hampered by the lack of technologies capable of producing the gram-kilogram amounts of minicircles required for pre-clinical and clinical trials. For example, the best volumetric productivities of minicircles obtained during the cell culture step reported in the literature are still only of the order of 0.5–9.0 mg/L (Kreiss et al. 1998; Chen et al. 2005; Mayrhofer et al. 2008; Kay et al. 2010; Gaspar et al. 2014). This offers a striking contrast with the developments observed in plasmid manufacturing, which have pushed fermentation productivities up to 2.2–2.6 g/L (Carnes et al. 2011; Gonçalves et al. 2014). The low performance of the fermentation processes used to produce minicircle could be ascribed to (i) low expression of recombinases (Bigger et al. 2001; Jechlinger et al. 2004), (ii) low recombinase activity in cells reaching stationary phase (Kay et al. 2010), and (iii) susceptibility of recombinases to changes in pH, temperature, and metabolite accumulation (Chen et al. 2005; Simcikova et al. 2014).

One aspect that has not been examined in the context of minicircle production is the role of messenger RNA (mRNA) secondary structure on the expression of the recombinase. This could be an important bottleneck since a number of authors have gathered evidence that points to the fact that gene expression in *E. coli* is inversely related to the stability of the secondary structure of their ribosome binding sites (RBS) (e.g., de Smit and van Duin 1990; Pfleger et al. 2005; Cèbe and Geiser 2006; Salis et al. 2009). The main goal of this study was to improve the performance of minicircle production by ParA resolvase-mediated in vivo recombination by focusing attention on the RBS and surrounding sequence of the mRNA of ParA (Smith and Schleif 1978). We reasoned that by changing the nucleotide sequence of this 5′ untranslated region (5′-UTR), potential hairpins that might be causing ribosomes to stall could be destabilized, thus increasing translation of mRNA and ParA levels and ultimately improving recombination of parental plasmids into minicircles. In our model system, the ParA resolvase was placed under the control of the arabinose-inducible P_{BAD}/araC promoter (Smith and Schleif 1978) and strains derived from BW27783, which was designed for improved uptake of arabinose (Khlebnikov et al. 2001), were used for parental plasmid production and recombination. Figure 1a shows the nucleotide sequence of the original araBAD regulatory region. The Pribnow (or −10 region) sequence TCTACT precedes the transcription start site of the

a

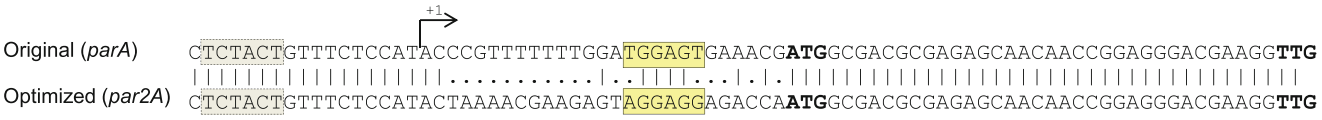

b

		mRNA (nt)	ΔG_{mRNA} (kcal/mol)	ΔG_{total} (kcal/mol)	TIR (AU)
16S rRNA	3′ – AUUCCUCCA – 5′	47	-6.3	1.56	1,236
parA mRNA	ACCCGUUUUUUUGGAUGGAGUGAAACG**AUG** …	57	-11.2	6.46	136
		67	-16.3	11.56	14
		77	-19.7	8.46	55
16S rRNA	3′ – AUUCCUCCA – 5′	47	-2.6	-7.04	59,285
par2A mRNA	ACUAAAACGAAGAGUAGGAGGAGACCA**AUG** …	57	-6.3	-3.34	11,214
		67	-6.3	-3.34	11,214
		77	-15.4	-0.74	3,480

c

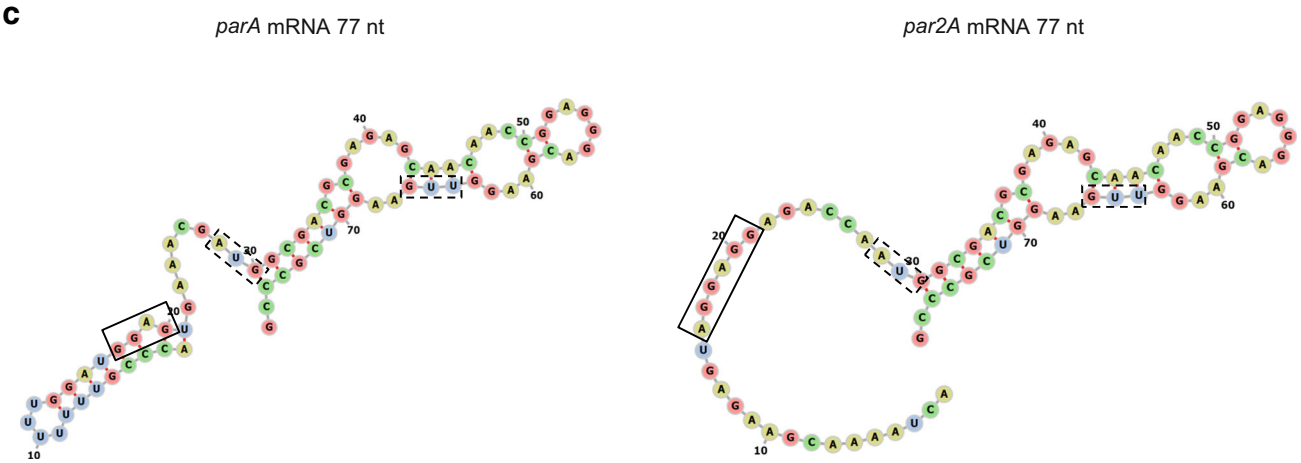

Fig. 1 **a** Nucleotide sequence of the P_{BAD} regulatory region showing the original (*parA*) and optimized (*par2A*) sequences. The start of the messenger RNA is designated position *+1*. Also shown are the characteristic Pribnow (or −10 region) sequence (*dashed box*) that precedes the *parA* mRNA, the RBS consensus (AGGAGG) sequence (*solid box*), and the ATG and TTG start codons (*in bold*). The optimized 5′-UTR was generated by the RBS calculator v2.0 (https://salislab.net/software/). The algorithm predicted an increase in the translation initiation rate (*TIR*) of 817-fold based on a 77-nucleotide-long mRNA subsequence including a 27-nucleotide 5′-UTR sequence. **b** Stability analysis of the translation initiation complex formed between mRNA subsequences containing the 5′-UTR plus 20, 30, 40, or 50 nucleotides and the 16S rRNA. Changes in Gibbs free energy were calculated according to Salis et al. 2009 and Borujeni et al. 2013 (Eq. 1). The values for $\Delta G_{spacing}$, ΔG_{start}, and $\Delta G_{standby}$ were similar for the original and optimized 5′-UTRs, whereas ΔG_{mRNA} depends on the size of the mRNA. *TIR* translational initiation rate, *AU* arbitrary units, *nt* nucleotides. **c** Predicted structures of the original and optimized *parA* transcripts encompassing the 5′-UTR (27 nt) and the first 50 nt. *Rectangular boxes* correspond to the AUG or UUG start codons (*dashed*) and to the Shine-Dalgarno sequence (*solid line*)

araBAD mRNA by 10 nucleotides. A 27-nucleotide-long *E. coli* 5′-UTR is then found that includes the Shine-Dalgarno (SD) sequence GGAG before the ATG start codon. The parA gene also contains an alternative TTG start codon at position 37. Both sites are used, generating ParA polypeptides with 24.2 and 22.7 kDa (Eberl et al. 1994).

Optimization of the 5′-UTR that precedes the first translational start site was performed on the basis of the equilibrium statistical thermodynamic model developed by Salis and coworkers (Salis et al. 2009). The model describes and quantifies the interaction between an mRNA transcript and the 30S ribosome complex, which includes the 16S ribosomal RNA (rRNA) and the transfer RNA^{fMet} ($tRNA^{fMet}$), by calculating

the change in Gibbs free energy upon assembly, ΔG_{total}, using an equation that accounts for five molecular interactions (Salis et al. 2009; Borujeni et al. 2013):

$$\Delta G_{total} = \Delta G_{mRNA-rRNA} - \Delta G_{mRNA} + \Delta G_{spacing} + \Delta G_{start} + \Delta G_{standby} \quad (1)$$

In this equation, $\Delta G_{mRNA:rRNA}$ accounts for hybridization and co-folding of the mRNA subsequence and 16S rRNA, ΔG_{mRNA} for the unfolding of the mRNA subsequence from its most stable secondary structure and ΔG_{start} for the hybridization of the start codon with the initiating tRNA anticodon loop. $\Delta G_{standby}$ and $\Delta G_{standby}$ are free energy penalties associated with the binding of the ribosome to the mRNA subsequence and with the non-optimal distancing between the 16S rRNA binding site and the start codon, respectively (Salis et al. 2009; Borujeni et al. 2013). These free energies and the secondary structures at the 5′-UTR of the encoding mRNAs were further analyzed using a web interface of the model, the RBS online calculator (https://salislab.net/software/). Production systems were then set up where the *parA* gene with the original or the optimized 5′-UTR (Fig. 1a) was inserted either in a low-copy number helper plasmid or in the chromosome of the host strain. The ability of the aforementioned systems to produce ParA resolvase was then compared by analyzing the amount of *parA* mRNA and ParA protein produced. Recombination efficiency studies were performed using a parental plasmid backbone (pMINI) that was constructed to generate green fluorescence protein (GFP)-expressing minicircles.

Material and methods

All primers used were purchased from Sigma-Aldrich (Boston, MA), with the exception of primers used for quantitative PCR (qPCR) and quantitative reverse transcriptase PCR (qRT-PCR) (STABvida, Portugal). The Phusion® High-Fidelity DNA Polymerase (New England Biolabs) was used to synthesize PCR fragments required for cloning. Colony PCR detection was performed with the HotStarTaq Master Mix Kit (Qiagen). Restriction enzymes were purchased from Promega. The anti-ParA antiserum was a kind from Prof. Helmut Schwab from Graz University of Technology.

Construction of BWAA, BW1P, and BW2P strains

The *E. coli* strain BW27783 [F-, *Δ(araD-araB)567*, *ΔlacZ4787*(::rrnB-3), λ^-, *Δ(araH-araF)570*(::*FRT*), *ΔaraEp-532*::*FRT*, φP_{cp8}*araE535*, *rph-1*, *Δ(rhaD-rhaB)568*, *hsdR514*], originally designed for improved arabinose uptake (Khlebnikov et al. 2001) was purchased from the Coli Genetic Stock Center (CGSC) at Yale (USA) and used to generate strains BWAA, BW1P, and BW2P as described next.

E. coli BWAA was obtained by knocking out the *endA* gene (responsible for non-specific degradation of plasmid DNA) and the *recA* gene (involved in homologous recombination) of the BW27783 strain by P1 transduction (Thomason et al. 2007) using donor strains (JW2912-1 and JW2669-1 from CGSC) of the Keio collection (Baba et al. 2006). These strains contain a kanamycin resistance cassette (Kan^R) flanked by FLP recognition target sites (FRT sites) that is designed to replace the target genes in the recipient strain. First, donor cells were infected by P1 phage and then harvested phage was used to transfect the recipient BW27783 cells. The kanamycin resistance gene was removed via the action of an FLP recombinase (Datsenko and Wanner 2000). The resulting BWAA strain was used to drive parental plasmid recombination via expression of ParA resolvase from the low-copy plasmids pMMBparA and pMMBpar2A.

E. coli strains BW1P and BW2P were designed to express ParA resolvase from a single chromosomal gene copy by disrupting the *endA* gene via the insertion of the P_{BAD}/*araC-parA* (BW1P) or P_{BAD}/*araC-RBS-parA* (BW2P) cassettes into the BW27783 chromosome.

BW1P was constructed using the large genomic insertion method of Kuhlman and Cox, which is based on double-stranded DNA breaks and λ-Red recombination (Kuhlman and Cox 2010). Briefly, the landing pad consisting of *tetA* tetracycline resistance gene flanked by the homing endonuclease I-*Sce*I recognition site, small 25-bp landing pad regions, and complementary regions of the desired *endA* integration site (underlined) was introduced into *E. coli* BW27783 host strain harboring pTKRED, a plasmid carrying the machinery required for the downstream steps. Primers LPfwd (CACGGAGTAAGTGATGTACCGTTATTTGTCTATTGCTGCGGTGGTACTGAGCTACGGCCCCAAGGTCCAAACGGTGA) and LPrev (TTAGCTCTTTCGCGCCTGGCAAGCGCGTTGCACATACGGGTTATGATTGGCTTCAGGGATGAGGCGCCATC) were used to amplify the landing pad by PCR using the pTKS/SC plasmid as a template. The positive colonies (spectinomycin and tetracycline resistant) carrying the landing pad inserted in the desired *endA* chromosomal location were transformed with the donor plasmid pTKIP*parA* carrying the P_{BAD}/*araC-parA* cassette flanked by the same 25-bp landing pad regions and I-*Sce*I recognition sequences. The incubation of positive colonies for 24 h in a medium with IPTG and L-arabinose induces the homing endonuclease, leading to the cleavage of both the donor plasmid and the chromosome at the site of the landing pad and the incorporation of the insertion fragment by λ-Red enzymes.

The BW2P strain was constructed by an adapted λ-Red recombination method as described by Datsenko and

Wanner (2000) since the results were not obtained with the method of Kuhlman and Cox (2010). Briefly, the cassette containing P_{BAD}/*araC-par2A* was amplified from template pTKIPpar2A using the Platinum PCR SuperMix (Invitrogen) and 300 nM of each of the primers par2Afwd (TCGAGGTCGACTGCCCGGC) and AraCSalIrev (TCCGTCAAGCCGTCGACTGTCTG), both of which contain *Sal*I restriction sites (underlined). The digested and gel-purified cassette was cloned into the *Sal*I restriction site of pKD13. The resulting plasmid was then used for amplification of the full recombination Kan cassette using 300 nM of each of the primers EndA_cass_for2: (ATCTGGCTGATTGCATACCAAAACAGCTTTCGCTACGTTGCTGGCTCGTTTTAACACGGAGTAAGTGATGGTGTAGGCTGGAGCTGCTTC) and EndAPar2Acasrev: (GTTGTACGCGTGGGGTAGGGGTTAACAAAAAGAATCCCGCTAGTGTAGGTTAGCTCTTTCGCGCCTGGCATTAATTCCGGGGATCCGTCG). The homology targeting of the *endA* in the genome is underlined. The amplified Kan cassette was used to transform electrocompetent host BW27783/pKD46, allowing homologous recombination. The kanamycin resistance gene was removed by a FLP recombinase expressed from plasmid pCP20 (Datsenko and Wanner 2000). The *recA* knockouts of the BW1P and the BW2P strains were then performed by the P1 transduction method previously described.

Plasmids pTKS/SC, pTKIP, and pTKRED (Kuhlman and Cox 2010) were obtained from Dr. Kuhlman in Princeton University.

Plasmids

Plasmid pVAXmini (5946 bp) was constructed as described previously (Simcikova et al. 2014). This plasmid contains a P_{BAD}/*araC-parA* cassette with the ParA resolvase gene under a P_{BAD} promoter and the *araC* repressor gene in the opposite direction, and two 133-bp-long multimer resolution sites (MRS) flanking the eukaryotic expression cassette (Fig. 2a). The parental plasmid backbone pMINI (4701 bp) was obtained from pVAXmini by deletion of the P_{BAD}/*araC-parA* region by *Sfi*I and *Eco*RV digestion (Fig. 2b). This plasmid was then used to transform *E. coli* strains BWAA/pMMBparA, BWAA/pMMBpar2A, BW1P, and BW2P. Plasmids pMMBparA (Fig. 2c) and pMMBpar2A were derived, as described below, from the low-copy number plasmid pMMB206, which was obtained from ATCC (ATCC® 37808™).

Ribosome binding site and surrounding sequence

The RBS online calculator (Salis et al. 2009; Borujeni et al. 2013; https://salislab.net/software/) was used in the forward engineering mode to design a 27-nucleotide-long 5′-UTR that would lead to an increase in the translational initiation rate (TIR) of ParA recombinase expressed from a low-copy number helper plasmid or from an integrated copy in the chromosome. An arbitrary 500–1000-fold increase of TIR was set as goal, and a 67-nucleotide-long mRNA, which included the 27 nucleotides of the 5′-UTR of parA mRNA and 40 nucleotides of the coding region, was used as input. The RBS online calculator was also used in a reverse engineering mode to predict the TIR of the original and optimized 5′-UTRs plus the first 20, 30, 40, and 50 nucleotides of the coding region.

The optimized 5′-UTR was synthesized and then introduced upstream of the *parA* gene by replacing the original RBS via SOEing PCR as described below. First, two similarly sized fragments overlapping a 27-bp region (underlined nucleotides) of the new 5′-UTR were synthetized by conventional PCR using pVAXmini as a template DNA and the following sets of primers: Spar2Afwd (CGAAGCAGGGATTCTGCAAAC) and Spar2Arev (TGGTCTCCTCCTACTCTTCGTTTTAGTATGGAGAAACAGTAGAGAGTTGCGA) or Spar2Bfwd (ACTAAAACGAAGAGTAGGAGGAGACCAATGGCGACGCGAGAGCAAC) and Spar2Brev (TGATAGCGGTCCGCCACA), respectively, amplifying

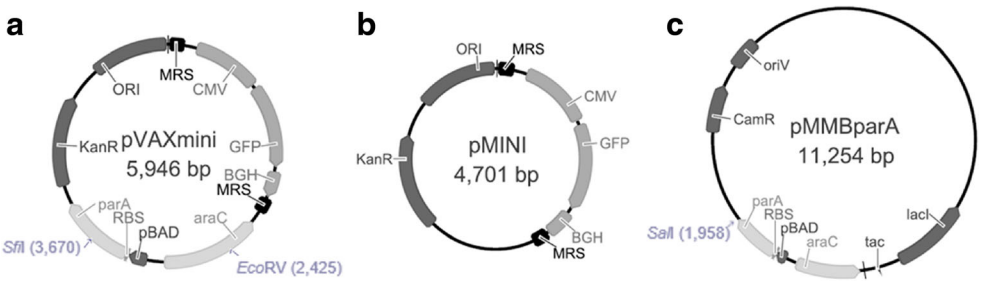

Fig. 2 Schematic diagram of plasmid backbones used in this work. **a** pVAXmini. **b** pMINI. c pMMBparA. *MRS* multimer resolution sites of the *parA* resolvase system, *CMV* cytomegalovirus immediate early promoter, *GFP*: green fluorescence protein gene, *BGH* bovine growth hormone polyadenylation signal, *AraC* repressor of arabinose operon, *pBAD* promoter of AraBAD, *RBS* ribosome binding site, *ParA* resolvase gene, *KanR* kanamycin resistance gene, *ORI* origin of replication, *CamR* chloramphenicol resistance gene, *oriV* IncQ replication origin, *tac* IPTG-inducible promoter, *LacI* repressor of lactose operon

fragments of 1283 and 1505 bp. In a second step, the two amplified fragments were annealed by the overlapping regions without primers to create a template for an additional PCR reaction with edge primers Spar2Afwd and Spar2Brev producing a 2761-bp amplicon containing the p_{BAD}/*araC-par2A* cassette. The arabinose promoter cassettes with the optimized and the original 5′-UTRs were respectively digested with *Sal*I and *Sal*I/*Sma*I and cloned into the low-copy number plasmid pMMB206 (9311 bp), thus generating plasmids pMMBparA (P_{BAD}/*araC-parA* cassette, see Fig. 2c) and pMMBpar2A (P_{BAD}/*araC-par2A* cassette) both with 11,254 bp.

Shake flask cultures

Five milliliters of Luria-Bertani (LB) medium supplemented with appropriate antibiotics (kanamycin, 30 μg/mL; chloramphenicol, 34 μg/mL) and 0.5 % (*w*/*v*) glucose were inoculated with a loop of −80 °C frozen *E. coli* cells harboring the parental plasmid pMINI and incubated overnight at 30 °C and 250 rpm. Next, an appropriate volume of this seed culture was used to inoculate 50 mL of LB medium with antibiotic to an optical density at 600 nm (OD_{600}) of 0.1. Cultures were then incubated at 37 °C and 250 rpm until reaching stationary phase. In a typical experiment, the transcription of *parA* resolvase was induced by adding 0.01 % (*w*/*v*) L-(+)-arabinose directly to the medium after 4 h of growth (early stationary phase) and recombination was allowed to proceed for 1–2 h. Specific volumes of culture samples withdrawn at different time points were centrifuged to obtain pellets with the same amount of cells that were stored at −20 °C for further analysis.

In order to prepare material for RT-PCR, qPCR, and Western blot analysis, strains BWAA/pMMBparA, BWAA/pMMBpar2A, BW1P, and BW2P were grown as described above using 100 mL of LB medium. After 5 h of growth, a specific volume of culture was centrifuged (6000*g*, 15 min) and cell pellets were stored at −20 °C until further analysis.

Bioreactor cultures

A pre-inoculum was prepared by transferring a loop of −80 °C frozen *E. coli* BW2P cells harboring the pMINI parental plasmid to 5 mL of complex medium [10 g/L bacto peptone, 10 g/L yeast extract, 3 g/L $(NH_4)_2SO_4$, 3.5 g/L K_2HPO_4, 3.5 g/L KH_2PO_4, 200 mg/L thiamine, 2 g/L $MgSO_4$, and 1 mL/L of a trace element solution (Listner et al. 2006)] supplemented with 30 μg/mL of kanamycin and 5 g/L glucose. Cells were grown overnight at 30 °C and 250 rpm. The next day, an inoculum was prepared by seeding 1 mL of the pre-inoculum in 100 mL of complex medium supplemented with 2 g/L glycerol. These cells were grown up to early exponential phase (OD_{600}~1.1) at 37 °C and 250 rpm. Batch fermentations were performed in a Fermac 360 Bioreactor (Electrolab) with a working volume of 1.1 L as described next. First, 1 L of complex medium was autoclaved in the bioreactor, and trace element solution, kanamycin (30 mg/L), and 40 g/L glycerol were added. Then, the bioreactor was inoculated to set the initial OD_{600} to 0.1. The dissolved oxygen set point was controlled at 30 % using an agitation cascade (200 to 800 rpm), and air was provided at a flow rate of 1 vvm. The pH was controlled at 7.1 using 2 M NaOH and 2 M H_2SO_4. Antifoam was manually added as required. Samples were taken periodically from the bioreactor to quantify biomass and plasmid DNA and to determine the parental plasmid recombination efficiency.

Analysis of plasmid recombination efficiency by densitometry

Plasmids were isolated with the Qiaprep Spin Miniprep Kit (Qiagen) according to the manufacturer's instructions. Total plasmid DNA (200 or 500 ng) was digested with *Sac*II, a restriction enzyme that has only one recognition site on the miniplasmid (MP) region of the parental pMINI plasmid (PP). Restriction mixtures were loaded onto 1 % agarose gels, and electrophoresis was carried out at 100 V, for 50 min, with TAE buffer (40 mM Tris base, 20 mM acetic acid and 1 mM EDTA, pH 8.0). The gels stained with ethidium bromide (1 μg/mL) were visualized with an Eagle Eye II image acquisition system from Stratagene (La Jolla, CA, USA). The intensity of the bands corresponding to linearized parental plasmid (I_{PP}) and miniplasmid MP (I_{MP}) measured using ImageJ software (Schneider et al. 2012) was then used to estimate the recombination efficiency (*Re*) according to the following equation:

$$Re\ (\%) = \frac{r_{Mw} I_{MP}}{I_{PP} + r_{Mw} I_{MP}} \times 100 \qquad (2)$$

where r_{Mw} (≈1.67) is the ratio of the sizes (hence of the molecular weights) of PP (4701 bp) and MP (2820 bp). This equation provides an approximate estimate of *Re* since it assumes that the intensity of the bands is proportional to mass and disregards the fact that MPs continue to replicate after recombination (Alves et al. 2016).

Determination of parA gene copy number

The number of copies of the *parA* gene in cells either in the chromosome or in the low-copy number plasmids was determined by performing by a "hot-start" SYBR Green I-based quantitative real-time PCR using the Roche LightCycler as described before (Carapuça et al. 2007). Primers parAfwd (CAGTACGGACGAGCAGAATC) and parArev (GGCTGATGCGGTCGATCTTC) were used at 0.5 μM final concentration, and tests were made with 50,000 or 300,000

E. coli cells. The 194-bp-long fragment was amplified with the following program: 10 min, 95 °C, 40× (10 s 95 °C, 5 s 55 °C, 7 s 72 °C). The threshold cycle (Cp) values were calculated by the LightCycler software version 4.1 (Roche Diagnostics) using the second derivative method. Mean Cp values and standard deviations were calculated from two independent assays. An identical methodology was used to quantify the reference 16S rRNA gene. Samples with 50,000 cells and sense (ACACGGTCCAGAACTCCTACG) and antisense (GCCGGTGCTTCTTCTGCGGGTAACGTCA) primers were used to amplify a 182-bp fragment.

Quantification of parA mRNA

Total RNA was extracted from *E. coli* cells (BWAA, BWAA harboring pMMBparA or pMMBpar2A, BW1P, and BW2P) with and without L-arabinose induction using the High Pure RNA Isolation Kit (Roche), following the manufacturer's instructions. For each RNA sample, 800 ng of total RNA (quantified using a NanoVue Plus spectrophotometer) was reverse transcribed using the 1st Strand cDNA Synthesis Kit for RT-PCR (AMV) (Roche), with primers parArev and rrsAfwd (GACGGGTGAGTAATGTCTGG) separately, following the manufacturer's instructions. Each cDNA sample was quantified by qPCR as described above using the set of primers parAfwd/parArev or rrsaAfwd/rrsarev (TCTTCATACAC GCGGCATGG) to amplify fragments of 194 or 308 bp within the *parA* or the reference 16S rRNA genes, respectively. Non-transformed BWAA was used as a negative control for *parA* expression.

Quantification of ParA resolvase

Firstly, BWAA transformed with either the pMMBparA or pMMBpar2A plasmid, and BW1P and BW2P strains were grown as described before. Cell pellets (OD_{600} = 200) were resuspended in 1 mL of a buffer containing 25 mM Tris, pH 8; 0.1 mM EDTA; 50 μM benzamidine; 100 μM PMSF; 1 mM 2-mercaptoethanol; 0.02 % brij58; and 1 M NaCl (Eberl et al. 1994) and sonicated at 30 W for 10 min on ice (Bandelin SONOPULS). The lysates were then clarified by centrifugation (6000*g* at 4 °C for 5 min) and pre-purified in Amicon Ultra-2 mL-50 kDa units followed by permeate concentration in Amicon Ultra-0.5 mL-10 kDa units (Merck Millipore) in order to increase the content of the sample in proteins within the 10–50 kDa range. Total protein concentration was determined using the Pierce BCA Protein Assay Kit (Thermo Fisher Scientific). Protein samples (20 or 30 μg of total protein respectively of samples obtained with *parA* expressed from helper plasmids or from the bacterial chromosome) were loaded into 15 % SDS-polyacrylamide gels. Proteins were then transferred to a PVDF membrane with a 0.22-μm pore size (Bio-Rad) by electroblotting at 200 mA for 1 h, using 25 mM Tris, 192 mM glycine, and 20 % (*v*/*v*) methanol, pH 8.3, as transfer buffer. The membrane was then blocked with Tris-buffered saline (TBS) (150 mM NaCl, 10 mM Tris, pH 7.4) containing 3 % (*w*/*v*) BSA for 1 h at 40 °C. After blocking, the membrane was rinsed in TBS and incubated overnight at 4 °C with an anti-ParA antiserum diluted 1:100 in TBS containing 0.5 % (*w*/*v*) BSA. Following washing with TBS (five changes during 30 min in total), the membrane was incubated for 2 h at room temperature with secondary antibody (HRP-goat anti-rabbit IgG (Sigma), diluted 1:20,000 in TBS containing 0.5 % (*w*/*v*) BSA) and washed as described before. For ParA detection, blots were incubated in TBS containing 0.05 % (*w*/*v*) 3, 3′-diaminobenzidine (Bio-Rad) and 0.09 % (*v*/*v*) hydrogen peroxide. Colorimetric reaction was stopped by washing with tap water, and blots were dried at room temperature. Blot image acquisition and densitometry analysis were performed using the Quantity One 1-D Analysis Software from Bio-Rad.

Results

Optimization of the 5′-UTR of ParA resolvase

The 4701 bp parental plasmid backbone pMINI (Fig. 2b) was used to generate GFP-expressing minicircles (1881 bp) upon ParA resolvase-mediated in vivo recombination between two multimer resolution sites (MRS). The system was designed to set the ParA resolvase expression under the control of the arabinose-inducible P_{BAD}/*araC* promoter. The 5′-UTR of the *parA* gene was then modified based on the equilibrium statistical thermodynamic model developed by Salis and co-workers (Salis et al. 2009), in an attempt to increase expression of ParA resolvase via the tuning of the accuracy and efficiency with which the translation of mRNA begins. The RBS online calculator (Salis et al. 2009; Borujeni et al. 2013) was used first in a reverse engineering mode to predict the translation initiation rate (TIR) of the 27 nucleotides of the 5′-UTR from the original P_{BAD}/*araC*-inducible system plus the first 40 nucleotides of the coding region (Fig. 1b). Then, the forward engineering mode of the calculator was used to design a 27-nucleotide (nt)-long 5′-UTR with a TIR arbitrarily set to be 500- to 1000-fold higher that the TIR obtained with the original 5′-UTR. From the multiple solutions generated by the software, an optimized 5′-UTR was selected with a TIR of 11,214 arbitrary units (AU), which compares with a TIR of 14 AU for the original 5′-UTR (Fig. 1a, b). This points to a 800-fold increase in TIR, which is likely to translate into the expression of larger amounts of ParA and hence more efficient minicircle recombination. Among other modifications, it is worth noticing that the TGGAGT Shine-Dalgarno sequence in the original parA mRNA was replaced by the consensus AGGAGG sequence in the optimized par2A mRNA (Fig. 1a, b).

Since the thermodynamic model (Eq. 1) explicitly depends on the free energy of the mRNA subsequence being analyzed, ΔG_{mRNA}, the ΔG_{total} and TIR calculated by the RBS calculator algorithm are affected by the size of the mRNA. Therefore, we considered four different sized mRNAs for the TIR predictions, which include 27 nucleotides from the 5′-UTR plus the first 20, 30, 40, or 50 nucleotides of the *parA* mRNA (Fig. 1b). Data concerning larger mRNAs sizes is not included in Fig. 1b since the corresponding ΔG_{total} and TIR values did not change significantly from the ones obtained with a 77-nt-long mRNA subsequence (see Fig. S1). The results show that TIR values are always higher (i.e., ΔG_{total} is always lower) when the mRNA subsequence contains the optimized 5′-UTR, no matter the size of the subsequence being analyzed (Fig. 1b).

The secondary structures of the mRNA subsequences with the original and optimized 5′-UTRs were further analyzed using the RBS online calculator. An observation of the most stable secondary structure obtained for the 77-nt-long mRNA subsequence with original 5′-UTR shows the presence of a long stem-loop structure that includes the Shine-Dalgarno region and is held in place by 21 base pairs, which could potentially interfere with ribosome binding and thwart *parA* expression (Fig. 1c). However, when the new 5′-UTR is introduced, a looser structure and less base pairing (13) are observed (Fig. 1c). The values of the predicted minimum free energy of folding of the mRNA subsequence, ΔG_{mRNA}, are also consistent with these observations, indicating an increase from −19.7 to −15.4 kcal/mol when moving from the original to the optimized 5′-UTR (Fig. 1b, c). Similar conclusions can be drawn from the analysis of the structures (see Fig. S2) and ΔG_{mRNA} (Fig. 1b) of mRNA subsequences with 47, 57, and 67 nt. Overall, the results indicate that the secondary structures obtained with the new 5′-UTR are less stable when compared with the original.

The predicted free energy changes associated with the assembly of the 30S ribosomal complex on the *parA* mRNA, ΔG_{total}, for sub-sequences with 47, 57, 67, and 77 nt vary between 1.56 and 11.56 kcal/mol (Fig. 1b). These values contrast with the predictions of ΔG_{total} for the *par2A* mRNA-rRNA complex, which varied between −7.04 and −0.74 kcal/mol.

The fact that ΔG_{total} of mRNA subsequences with the optimized 5′-UTR is lower and negative indicates the presence of attractive interactions between the ribosome and mRNA, whereas the larger ΔG_{total} obtained with the original 5′-UTR (1.56–11.56 kcal/mol) points to a less stable complex, hence less efficient translation of ParA. This is reflected in the predicted TIR values, which varied between 14 and 1236 AU for parA mRNAs and from 3480 and 59,285 AU for par2A mRNAs (Fig. 1b).

Expression of ParA from low-copy number plasmids

P_{BAD}/*araC-parA* cassettes with original and optimized 5′-UTRs (Fig. 1) were introduced in the low-copy number plasmid pMMB206 (Morales et al. 1991) to generate plasmids pMMBparA (Fig. 2c) and pMMBpar2A, respectively. These helper plasmids were then used to drive ParA resolvase expression and recombination of parental plasmid pMINI (Fig. 2b) in *E. coli* BWAA. This strain was derived from *E. coli* BW27783—a strain improved for arabinose uptake—by knocking out the *endA* and *recA* genes to minimize non-specific digestion and recombination of pDNA (Phue et al. 2008; Gonçalves et al. 2013) and thus assure the maintenance of the supercoiled isoform of minicircle molecules produced. The number of pMMBparA and pMMBpar2A copies per transformed BWAA cell was determined by qPCR to be around 14/cell, a number which is consistent with the 12–13 copies of the pMMB206 reported in the literature (Morales et al. 1991).

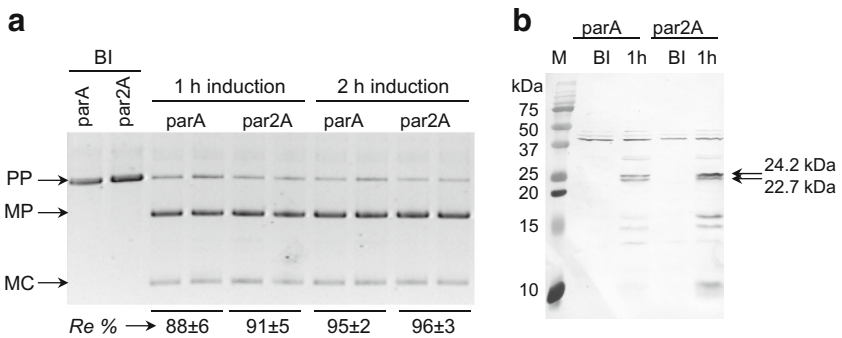

Fig. 3 Minicircle recombination driven by expression of ParA resolvase from low-copy number plasmids harboring *parA* with original (parA) and optimized (par2A) 5′-UTRs. Minicircle recombination was induced at the early stationary phase, after 4 h of cell growth (equivalent to C in Fig. 4). **a** Agarose gel electrophoresis analysis of cells collected before (*BI*) and after 1 and 2 h of induction. Three independent experiments were performed in duplicate. The recombination efficiencies (*Re*) obtained from low-copy number plasmids pMMBparA and pMMBpar2A were not statistically different ($p > 0.05$). *PP* parental plasmid, *MP* miniplasmid, *MC* minicircle. **b** Western blot analysis showing expression of ParA resolvase with original (*parA*) and optimized (*par2A*) 5′-UTRs, before (*BI*) and after 1 h of induction

A tight control of ParA resolvase expression and recombination of pMINI was successfully obtained in the BWAA/pMMBparA and BWAA/pMMBpar2A systems, as can be seen from an agarose gel electrophoresis analysis (Fig. 3a). Parental plasmids recombined into the corresponding minicircle and miniplasmid species only upon arabinose addition, with efficiencies of 88–91 and 95–96 % after 1 and 2 h, respectively. This constitutes an improvement over the recombination yields of 50 % obtained by Jechlinger et al. (2004) when expressing ParA under P_{BAD}/*araC* control from a low-copy number plasmid. However, the modification introduced in the translational initiation region did not result in a significant improvement in the recombination efficiency, as seen in Fig. 3a. This indicates that in these systems, the TIR obtained with the original 5′-UTR is sufficient to produce enough ParA resolvase to reach maximum plasmid recombination. The results of a Western blot performed on samples obtained before and after induction of *parA* expression with arabinose are shown in Fig. 3b. The samples obtained before induction displayed almost no reactivity with a ParA antiserum (Fig. 3b). However, after 1 h of arabinose induction, bands corresponding to the 24.2 and 22.7 kDa polypeptides encoded in *parA*, corresponding to the two start codons (Eberl et al. 1994), are clearly seen (Fig. 3b). Pairs of bands around the 15 and 10 kDa regions are also seen that can be attributed to cleavage of the ParA-22.7 and ParA-24.2 proteins. A comparison between the ParA expression levels, based on the densitometry of the Western blots, showed a 1.7 ± 0.8-fold (two independent experiments) higher translation driven by the pMMBpar2A plasmid. The higher density of the ParA-24.2 band relative to the ParA-22.7 band (Fig. 3b) can be explained by noting that the par2A mRNA-rRNA complex is more stable if the ATG start codon is used (TIR = 3480 AU) instead of the alternative TTG codon (TIR = 261 AU). For the parA mRNA-rRNA complex, the difference between the TIR obtained with the ATG codon (TIR = 55 AU) and the alternative TTG codon (TIR = 323 AU) is less pronounced, and thus the amounts of the ParA-24.2 and ParA-22.7 are similar (Fig. 3b).

Expression of ParA from the chromosome

Minicircle production systems were set up to drive ParA resolvase-mediated recombination of parental plasmid pMINI from a single gene copy of *parA* stably inserted in the *E. coli* chromosome. Namely, the BW1P and BW2P strains were constructed by the insertion of the cassettes P_{BAD}/*araC-parA* and P_{BAD}/*araC-par2A*, respectively. The performance of the two strains was examined in a series of shake flask experiments. Induction was performed by adding 0.01 % (*w*/*v*) of L-arabinose at different stages of the late growth phase (marked as A, B, and C in Fig. 4a), at a time when large amounts of cells and parental plasmid are available. The pMINI recombination efficiency obtained after 1 h of arabinose addition varied significantly between the two strains (Fig. 4b). While the BW2P cells were able to rapidly express a sufficient amount of ParA resolvase to obtain 100 % of recombination after 1 h of induction at time point A, only 70 % of parental plasmid recombined into miniplasmid and minicircle when using strain BW1P under equivalent conditions (Fig. 4b). Recombination efficiencies were also higher for strain BW2P if arabinose induction was performed later at time points B and C (Fig. 4b). A substantial decrease in recombination was observed when cells were induced at growth stages closer to the stationary phase (Fig. 4b), with efficiencies

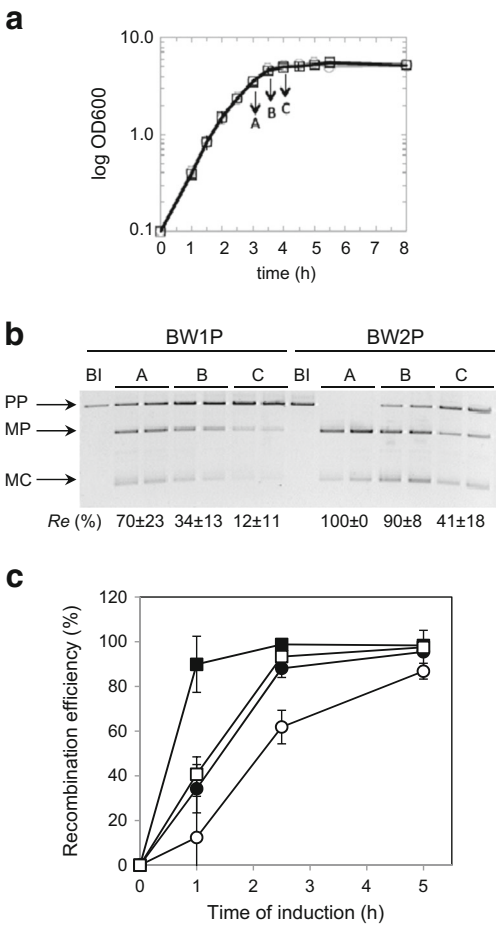

Fig. 4 Minicircle recombination driven by ParA resolvase expressed from a single copy of *parA* with original (*parA*) and optimized (*par2A*) 5′-UTRs harbored in the chromosome of *E. coli*. **a** Growth curve of *E. coli* BW2P/pMINI (*squares*) and BW1P/pMINI (*circles*) in 50 mL LB medium were induced when reaching specific growth phase *A*, OD_{600} 3.4–3.8; *B*, OD_{600} 4.4–4.8; and *C* OD_{600} = 5.0–5.2. **b** Agarose gel electrophoresis analysis of recombination efficiency after 1 h of induction with 0.01 % L-arabinose at different growth phases (*A*, *B*, and *C*). **c** Time course of recombination efficiency when induction started in growth phase B (*filled symbols*) or in growth phase C (*empty symbols*) of *E. coli* cells BW1P (*circles*) and BW2P (*squares*) harboring pMINI. The recombination efficiency with standard deviation results from densitometry analysis of 200 ng of linearized pDNA from at least three independent experiments

falling when moving from induction at point A to point C from 70 to 12 % for strain BW1P and from 100 to 41 % for strain BW2P (Fig. 4b).

A time course analysis of recombination showed that efficiencies close to 100 % could be obtained by inducing cells that were entering the stationary phase with both strains (95 % for BW1P and 98 % for BW2P), as long as the induction phase was extended to 300 min (Fig. 4c, time point B). Still, if induction was performed later in the early stationary phase, complete pMINI recombination was only observed for the BW2P strain (Fig. 4, time point C). These results show that the improvements made in the 5′-UTR of the *parA* gene in strain BW2P effectively led to a more accurate and efficient translation of the corresponding mRNA and hence to pMINI recombination efficiencies close to 100 %. Attempts to detect ParA by Western blot analysis were unfruitful, most likely due to the low levels of expression afforded by the single gene copy of *parA* in BW1P and BW2P.

Quantification of parA mRNA

The expression of ParA resolvase in the *E. coli* strains BWAA/pMMBparA, BWAA/pMMBpar2A, BW1P, and BW2P was further investigated by qRT-PCR using the BWAA strain as a negative control and the 16S rRNA gene as a reference (Fig. 5). In the absence of L-arabinose induction, the levels of *parA* mRNA were negligible across the different expression systems (Fig. 5). Upon L-arabinose induction, however, the levels of *parA* mRNA increased significantly. Furthermore, the systems with the original and the optimized 5′-UTRs located in helper plasmids produced a significantly higher amount of *parA* mRNA when compared to the corresponding system expressing ParA from a single copy in the bacterial chromosome: mRNA levels were 22-fold higher in BWAA/pMMBparA relatively to BW1P and 45-fold higher in BWAA/pMMBpar2A relatively to BW2P. Similar amounts of the 16S rRNA reference gene were obtained in all samples analyzed, and no *parA* mRNA was detected in the control BWAA strain, validating the data obtained (Fig. 5).

The results also show that (i) the amount of par2A mRNA in the BWAA/pMMBpar2A strain was 2.5-fold higher than the amount of parA mRNA in the BWAA/pMMBparA strain and that (ii) the amount of par2A mRNA in the BW2P strain was 1.6-fold higher than the amount of parA mRNA in the BW1P strain (Fig. 5).

Discussion

The expression of ParA resolvase under regulation of P_{BAD}/araC was chosen as arabinose is an effective inducible system for ParA and other recombinases in minicircle production (e.g., Kay et al. 2010; Jechlinger et al. 2004; Mayrhofer et al. 2005; Kobelt et al. 2013). The performance of minicircle production in *E. coli* by ParA resolvase-mediated in vivo recombination was optimized by manipulating the 5′-UTR of the *parA* mRNA. The starting hypothesis behind this approach was that the stability of the secondary structure of the RBS and surrounding sequence of *parA* could be compromising the expression of ParA and hence recombination.

In the first part of this work, a 27-nucleotide-long 5′-UTR potentially enabling a higher translation initiation rate was designed using the predictive thermodynamic model of Salis and co-workers (Salis et al. 2009) (Fig. 1). An analysis of original and optimized mRNA subsequences, which included the 5′-UTR and the first 20, 30, 40, or 50 nucleotides of the

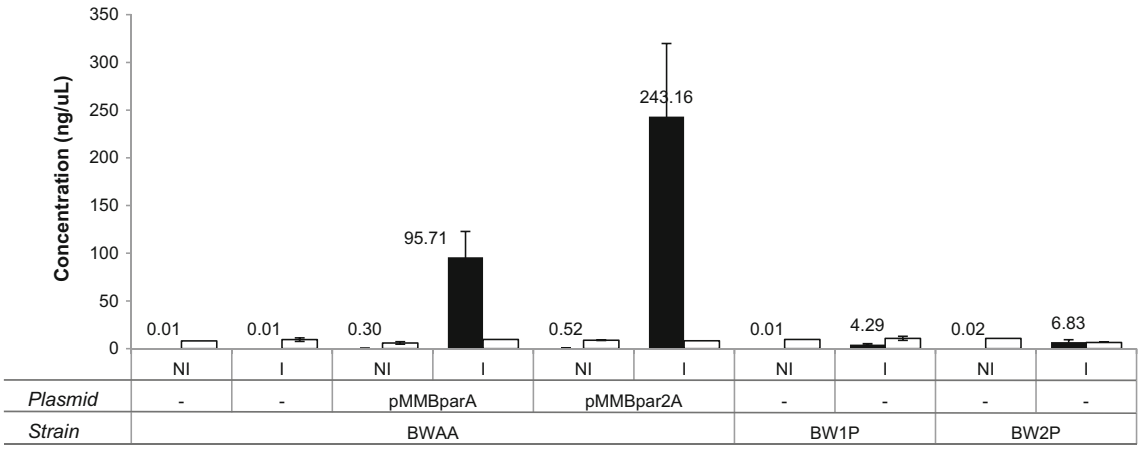

Fig. 5 Quantitative RT-PCR analysis of *parA* mRNA levels (*black bars*) in systems harboring the original or optimized 5′-UTRs located in helper plasmids (BWAA/pMMBparA and BWAA/pMMBpar2A) or in the bacterial chromosome (BW1P and BW2P). The results are shown for non-induced (*NI*) and arabinose-induced (*I*) cells. The non-transformed BWAA *E. coli* strain was used as a negative control for *parA* expression. Levels of expression of the reference gene 16S rRNA are also shown (*white bars*). Analyses were performed on samples containing 800 ng of total RNA extracted. Mean concentrations and standard deviations were obtained from two to four experiments

parA transcripts, predicted that the change in Gibbs free energy upon assembly of the 30S ribosome complex with the mRNA subsequences, ΔG_{total}, is lower with the new 5′-UTR. This indicates a more stable mRNA-rRNA complex and consequently higher translation initiation rates (Fig. 1b) (Salis et al. 2009; Borujeni et al. 2013).

The construction of the strains BWAA, BW1P, and BW2P, with enhanced uptake for the arabinose inducer (Khlebnikov et al. 2001) and deficiency in *end*A and *rec*A genes that increases the amount and the quality of pDNA (Phue et al. 2008; Gonçalves et al. 2013), was essential for a higher minicircle production. When ParA was expressed from low-copy number plasmids in the BWAA strain, full recombination of the model parental plasmid pMINI was obtained within 2 h, but no effect of the 5′-UTR was detected (Fig. 3). These results can be explained by assuming that the 14 copies/cell of the helper plasmids promote the transcription of an amount of mRNA that is sufficient to drive the expression of the ParA required for full recombination, even with a non-optimal 5′-UTR. This efficient recombination was also observed in other systems using several copies of the gene encoding the recombinase (Jechlinger et al. 2004; Chen et al. 2005; Mayrhofer et al. 2005; Kay et al. 2010) but not when driven by one single copy gene of the recombinase (Darquet et al. 1999; Bigger et al. 2001).

In spite of the good results obtained in terms of recombination efficiency, systems that rely on helper plasmids are clearly disadvantageous from the point of view of minicircle purification due the presence of additional plasmid species in process streams. This can also be inferred from the efforts made by researchers in locating the recombinase producing system either in the bacterial backbone of parental plasmids (e.g., Chen et al. 2005) or in the bacterial genome (e.g., Kay et al. 2010), although the main objective in these studies was the improvement of parental plasmid recombination. As an alternative minicircle production system, the *parA* gene was introduced in the bacterial chromosome of *E. coli*. In this case, cells with the optimized 5′-UTR performed clearly better in terms of recombination when compared to cells with the original 5′-UTR (Fig. 4).

A comparison of the two producer systems clearly indicates that recombination of pMINI proceeded faster when ParA was expressed from helper plasmids (compare Fig. 3 and C growth phase of Fig. 4), a fact that can be ascribed to the presence of higher levels of ParA. This observation is consistent with the fact that cells containing the helper plasmids have 14-fold more *parA* gene copies than cells with a single copy of *parA* in the genome and that induced cells produce significantly higher levels of *parA* mRNA when *parA* is expressed from helper plasmids (Fig. 5). A Western blot analysis failed to detect the presence of ParA when expression was driven from the chromosome (data not shown), providing further confirmation that systems relying on helper plasmids produce larger amounts of ParA (Fig. 3b). Nevertheless, the amount of resolvase obtained from a single *parA* copy inserted into the bacterial chromosome was sufficient to assure 100 % of recombination in a short time period, if the optimized 5′-UTR and an appropriate induction time point was chosen (see lane A for BW2P in Fig. 4b).

The increase in the amounts of ParA obtained with the optimization of the 5′-UTR was initially ascribed to a higher structural stability of the mRNA-rRNA complex and hence to a higher rate of translation. However, the fact that larger amounts of the optimized *parA* mRNA were observed both in the one-copy and 14-copy *parA* systems (Fig. 5) may indicate that the new 5′-UTR mRNA structure is probably (Hsu et al. 2006; Berg et al. 2009; Goldman et al. 2009) (i) increasing the stability of the complex RNA polymerase-transcript and thus reducing the amounts of abortive transcripts, (ii) decreasing the susceptibility to degradation of the transcript, and (iii) decreasing the availability to degradation because the transcript binds longer to rRNA. Thus, the final amount of the resolvase in the system is a compromise between transcriptional and translational rates.

Preliminary cultivation experiments in 1-L bioreactors indicate that cell densities of OD_{600}~40, recombination efficiencies of ~80 %, and volumetric titers of 50 mg/L total plasmid can be obtained with the optimized BW2P strain. Additional work is currently ongoing in order to optimize this process and thus take full advantage of the BW2P cells. Another hurdle in minicircle manufacturing, which is not addressed here, is linked to the problematic purification of minicircles from miniplasmids and un-recombined parental plasmids. Nevertheless, in parallel development, we have shown that minicircles recombined in BW2P cells can be obtained virtually free from nucleic acid impurities by resorting to a nicking endonuclease-assisted purification method (Alves et al. 2016).

In conclusion, this study highlights the importance of engineering the 5′-UTR upstream of the recombinase gene, which resulted in an optimization of the RBS and surrounding sequence of ParA resolvase. In contrast to previous studies (Darquet et al. 1997; Darquet et al. 1999; Kreiss et al. 1998; Bigger et al. 2001; Kay et al. 2010), insertion of a single copy of the optimized recombinase producing system in the bacterial genome (*E. coli* BW2P strain) proved to be efficient to drive sufficient recombinase expression for complete parental plasmid recombination.

Acknowledgments This work was supported by the MIT-Portugal Program, Fundação para a Ciência e a Tecnologia (grant UID/BIO/04565/2013 awarded to iBB—Institute for Bioengineering and Biosciences and PhD grant SFRH/BD/33786/2009 to Michaela Šimčíková).

Compliance with ethical standards This article does not contain any studies with human participants or animals performed by any of the authors.

Conflict of interest The authors declare that they have no conflict of interest.

References

Alves CP, Simcikova M, Brito L, Monteiro GA, Prazeres DMF (2016) Development of a nicking endonuclease-assisted method for the purification of minicircles. J Chromat A 1443:136–144. doi:10.1016/j.chroma.2016.03.035

Azzoni AR, Ribeiro SC, Monteiro GA, Prazeres DMF (2007) The impact of polyadenylation signals on plasmid nuclease-resistance and transgene expression. J Gene Med 9:392–402. doi:10.1002/jgm.1031

Baba T, Ara T, Hasegawa M, Takai Y, Okumura Y, Baba M, Datsenko KA, Tomita M, Wanner BL, Mori H (2006) Construction of *Escherichia coli* K-12 in-frame, single-gene knockout mutants: the Keio collection. Mol Syst Biol 2:2006.0008. doi:10.1038/msb4100050

Berg L, Lale R, Bakke I, Burroughs N, Valla S (2009) The expression of recombinant genes in *Escherichia coli* can be strongly stimulated at the transcript production level by mutating the DNA-region corresponding to the 5-untranslated part of mRNA. Microb Biotechnol 2:379–389. doi:10.1111/j.1751-7915.2009.00107.x

Bert AG, Burrows J, Osborne CS, Cockerill PN (2000) Generation of an improved luciferase reporter gene plasmid that employs a novel mechanism for high-copy replication. Plasmid 44:173–182. doi:10.1006/plas.2000.1474

Bigger BW, Tolmachov O, Collombet JM, Fragkos M, Palaszewski I, Coutelle C (2001) An araC-controlled bacterial cre expression system to produce DNA minicircle vectors for nuclear and mitochondrial gene therapy. J Biol Chem 276:23018–23027. doi:10.1074/jbc.M010873200

Borujeni AE, Channarasappa AS, Salis HM (2013) Translation rate is controlled by coupled trade-offs between site accessibility, selective RNA unfolding and sliding at upstream standby sites. Nucleic Acids Res 42:2646–2659. doi:10.1093/nar/gkt1139

Carapuça E, Azzoni AR, Prazeres DMF, Monteiro GA, Mergulhão FJM (2007) Time-course determination of plasmid content in eukaryotic and prokaryotic cells using real-time PCR. Mol Biotechnol 37:120–126. doi:10.1007/s12033-007-0007-3

Carnes AE, Luke JM, Vincent JM, Schukar A, Anderson S, Hodgson CP, Williams JA (2011) Plasmid DNA fermentation strain and process-specific effects on vector yield, quality, and transgene expression. Biotechnol Bioeng 108:354–363. doi:10.1002/bit.22936

Cèbe R, Geiser M (2006) Rapid and easy thermodynamic optimization of the 5′-end of mRNA dramatically increases the level of wild type protein expression in *Escherichia coli*. Protein Exp Purif 45:374–380. doi:10.1016/j.pep.2005.07.007

Chen ZY, He CY, Ehrhardt A, Kay MA (2003) Minicircle DNA vectors devoid of bacterial DNA result in persistent and high-level transgene expression *in vivo*. Mol Ther 8:495–500. doi:10.1016/S1525-0016(03)00168-0

Chen ZY, He CY, Meuse L, Kay MA (2004) Silencing of episomal transgene expression by plasmid bacterial DNA elements *in vivo*. Gene Ther 11:856–864. doi:10.1038/sj.gt.3302231

Chen ZY, He CY, Kay MA (2005) Improved production and purification of minicircle DNA vector free of plasmid bacterial sequences and capable of persistent transgene expression *in vivo*. Hum Gene Ther 16:126–131. doi:10.1089/hum.2005.16.126

Chen ZY, Riu E, He CY, Xu H, Kay MA (2008) Silencing of episomal transgene expression in liver by plasmid bacterial backbone DNA is independent of CpG methylation. Mol Ther 16:548–556. doi:10.1038/sj.mt.6300399

Chen Z, Cao J, Liao X, Ke J, Zhu S, Zhao P, Qi Z (2011) Plasmids enriched with CpG motifs activate human peripheral blood mononuclear cells *in vitro* and enhance th-1 immune responses to hepatitis B surface antigen in mice. Viral Immunol 24:199–209. doi:10.1089/vim.2010.0116

Darquet AM, Cameron B, Wils P, Scherman D, Crouzet J (1997) A new DNA vehicle for nonviral gene delivery: supercoiled minicircle. Gene Ther 4:1341–1349. doi:10.1038/sj.gt.3300540

Darquet AM, Rangara R, Kreiss P, Schwartz B, Naimi S, Delaère P, Crouzet J, Scherman D (1999) Minicircle: an improved DNA molecule for *in vitro* and *in vivo* gene transfer. Gene Ther 6:209–218. doi:10.1038/sj.gt.3300816

Datsenko KA, Wanner BL (2000) One-step inactivation of chromosomal genes in *Escherichia coli* K-12 using PCR products. Proc Natl Acad Sci U S A 97:6640–6645. doi:10.1073/pnas.120163297

de Smit MH, van Duin J (1990) Secondary structure of the ribosome binding site determines translational efficiency: a quantitative analysis. Proc Natl Acad Sci U S A 87:7668–7672

Dean DA, Strong DD, Zimmer WE (2005) Nuclear entry of nonviral vectors. Gene Ther 12:881–890. doi:10.1038/sj.gt.3302534

Eberl L, Kristensen CS, Givskov M, Grohmann E, Gerlitz M, Schwab H (1994) Analysis of the multimer resolution system encoded by the parCBA operon of broad-host-range plasmid RP4. Mol Microbiol 12:131–141. doi:10.1111/j.1365-2958.1994.tb01002.x

EMA-European Medicines Evaluation Agency 2001 ICH Topic Q6b. Note for guidance on quality, preclinical and clinical aspects of gene transfer medicinal products (CPMP/BWP/3088/99). London

Faurez F, Dory D, Le Moigne V, Gravier R, Jestin A (2010) Biosafety of DNA vaccines: New generation of DNA vectors and current knowledge on the fate of plasmids after injection. Vaccine 28:3888–3895. doi:10.1016/j.vaccine.2010.03.040

Gaspar VM, Maia CJ, Queiroz JA, Pichon C, Correia IJ, Sousa F (2014) Improved minicircle DNA biosynthesis for gene therapy applications. Hum Gene Ther 25:93–105. doi:10.1089/hgtb.2013.020

Goldman SR, Ebright RH, Nickels BE (2009) Direct detection of abortive RNA transcripts *in vivo*. Science 324:927–928. doi:10.1126/science.1169237

Gonçalves GAL, Prazeres DMF, Monteiro GA, Prather KLJ (2013) De novo creation of MG1655-derived *E. coli* strains specifically designed for plasmid DNA production. App. Microbiol Biotechnol 97:611–620. doi:10.1007/s00253-012-4308-5

Gonçalves GA, Prather KL, Monteiro GA, Carnes AE, Prazeres DMF (2014) Plasmid DNA production with *Escherichia coli* GALG20, a *pgi*-gene knockout strain: fermentation strategies and impact on downstream processing. J Biotechnol 186:119–127. doi:10.1016/j.jbiotec.2014.06.008

Hsu LM, Cobb IM, Ozmore JR, Khoo M, Nahm G, Xia L, Bao Y, Ahn C (2006) Initial transcribed sequence mutations specifically affect promoter escape properties. Biochemistry 45:8841–8854. doi:10.1021/bi060247u

Jechlinger W, Tabrizi CA, Lubitz W, Mayrhofer P (2004) Minicircle DNA immobilized in bacterial ghosts: *in vivo* production of safe non-viral DNA delivery vehicles. J Mol Microbiol Biotechnol 8:222–231. doi:10.1159/000086703

Kay MA, He CY, Chen ZY (2010) A robust system for production of minicircle DNA vectors. Nat Biotechnol 28:1287–1289. doi:10.1038/nbt.1708

Khlebnikov A, Datsenko KA, Skaug T, Wanner BL, Keasling JD (2001) Homogeneous expression of the PBAD promoter in *Escherichia coli* by constitutive expression of the low-affinity high-capacity AraE transporter. Microbiology 147:3241–3247. doi:10.1099/00221287-147-12-3241

Kobelt D, Schleef M, Schmeer M, Aumann J, Schlag PM, Walther W (2013) Performance of high quality minicircle DNA for *in vitro* and *in vivo* gene transfer. Mol Biotechnol 53:80–89. doi:10.1007/s12033-012-9535-6

Kreiss P, Cameron B, Darquet AM, Scherman D, Crouzet J (1998) Production of a new DNA vehicle for gene transfer using site-specific recombination. Appl Microbiol Biotechnol 49:560–567. doi:10.1007/s002530051213

Kreiss P, Cameron B, Rangara R, Mailhe P, Aguerre-Charriol O, Airiau M, Scherman D, Crouzet J, Pitard B (1999) Plasmid DNA size does not affect the physicochemical properties of lipoplexes but modulates gene transfer efficiency. Nucleic Acids Res 27:3792–3798. doi:10.1093/nar/27.19.3792

Kuhlman TE, Cox EC (2010) Site-specific chromosomal integration of large synthetic constructs. Nucleic Acids Res 38:e92. doi:10.1093/nar/gkp1193

Lechardeur D, Sohn KJ, Haardt M, Joshi PB, Monck M, Graham RW, Beatty B, Squire J, O'Brodovich H, Lukacs GL (1999) Metabolic instability of plasmid DNA in the cytosol: a potential barrier to gene transfer. Gene Ther 6:482–497. doi:10.1038/sj.gt.3300867

Lemp NA, Hiraoka K, Kasahara N, Logg CR (2012) Cryptic transcripts from a ubiquitous plasmid origin of replication confound tests for cis-regulatory function. Nucleic Acids Res 40:7280–7290. doi:10.1093/nar/gks451

Listner K, Bentley LK, Chartrain M (2006) A simple method for the production of plasmid DNA in bioreactors. Methods Mol Med 127:295–309. doi:10.1385/1-59745-168-1:295

Lu J, Zhang F, Xu S, Fire AZ, Kay MA (2012) The extragenic spacer length between the 5′ and 3′ ends of the transgene expression cassette affects transgene silencing from plasmid-based vectors. Mol Ther 20:2111–2119. doi:10.1038/mt.2012.65

Mayrhofer P, Tabrizi CA, Walcher P, Haidinger W, Jechlinger W, Lubitz W (2005) Immobilization of plasmid DNA in bacterial ghosts. J Control Release 102:725–735. doi:10.1016/j.jconrel.2004.10.026

Mayrhofer P, Blaesen M, Schleef M, Jechlinger W (2008) Minicircle-DNA production by site specific recombination and protein-DNA interaction chromatography. J Gene Med 10:1253–1269. doi:10.1002/jgm.1243

Mayrhofer P, Schleef M, Jechlinger W (2009) Use of minicircle plasmids for gene therapy. Methods Mol Biol 542:87–104. doi:10.1007/978-1-59745-561-9_4

Morales VM, Bäckman A, Bagdasarian M (1991) A series of wide-host-range low-copy-number vectors that allow direct screening for recombinants. Gene 97:39–47. doi:10.1016/0378-1119(91)90007-X

Pfleger BF, Fawzi NJ, Keasling JD (2005) Optimization of DsRed production in *Escherichia coli*: effect of ribosome binding site sequestration on translation efficiency. Biotechnol Bioeng 92:553–558. doi:10.1002/bit.20630

Phue J-N, Lee SJ, Trinh L, Shiloach J (2008) Modified *Escherichia coli* B (BL21), a superior producer of plasmid DNA compared with *Escherichia coli* K (DH5a). Biotechnol Bioeng 101(4):831–836. doi:10.1002/bit.21973

Salis HM, Mirsky EA, Voigt CA (2009) Automated design of synthetic ribosome binding sites to control protein expression. Nat Biotechnol 27:946–950. doi:10.1038/nbt.1568

Salyers AA, Gupta A, Wang Y (2004) Human intestinal bacteria as reservoirs for antibiotic resistance genes. Trends Microbiol 12:412–416. doi:10.1016/j.tim.2004.07.004

Schneider CA, Rasband WS, Eliceiri KW (2012) NIH Image to ImageJ: 25 years of image analysis. Nat Methods 9:671–675. doi:10.1038/nmeth.2089

Simcikova M, Prather KLJ, Prazeres DMF, Monteiro GA (2014) On the dual effect of glucose during production of pBAD/AraC based minicircles. Vaccine 32:2843–2846. doi:10.1016/j.vaccine.2014.02.035

Smith BR, Schleif R (1978) Nucleotide sequence of the L-arabinose regulatory region of *Escherichia coli* K12. J Biol Chem 253:6931–6933

Thomason LC, Costantino N, Court DL (2007) *E. coli* genome manipulation by P1 transduction. Curr Prot Mol Biol 1(17):1–1.17.8. doi:10.1002/0471142727.mb0117s79

USFDA-United States Food and Drug Administration (2007) Guidance for industry: Considerations for plasmid DNA vaccines for preventive infectious disease indications. Rockville

Wang Z, Troilo PJ, Wang X, Griffiths TG, Pacchione SJ, Barnum AB, Harper LB, Pauley CJ, Niu Z, Denisova L, Follmer TT, Rizzuto G, Ciliberto G, Fattori E, Monica NL, Manam S, Ledwith BJ (2004) Detection of integration of plasmid DNA into host genomic DNA following intramuscular injection and electroporation. Gene Ther 11:711–721. doi:10.1038/sj.gt.3302213

Yew NS, Zhao H, Przybylska M, Wu IH, Tousignant JD, Scheule RK, Cheng SH (2002) CpG-depleted plasmid DNA vectors with enhanced safety and long-term gene expression in vivo. Mol Ther 5:731–738. doi:10.1006/mthe.2002.0598

Zhao H, Hemmi H, Akira S, Cheng SH, Scheule RK, Yew NS (2004) Contribution of Toll-like receptor 9 signaling to the acute inflammatory response to nonviral vectors. Mol Ther 9:241–248. doi:10.1016/j.ymthe.2003.11.012